Available online at www.sciencedirect.com
ScienceDirect
Metabolism Clinical and Experimental 58 (2009) 934 – 945
Metabolism
Clinical and Experimental
www.metabolismjournal.com

Effects of pyridoxamine (K-163) on glucose intolerance and obesity in high-fat diet C57BL/6J mice

Shinji Hagiwara[a,c], Tomohito Gohda[a], Mitsuo Tanimoto[a], Takamichi Ito[a], Maki Murakoshi[a], Ikko Ohara[a], Takahiko Yamazaki[a], Masakazu Matsumoto[a], Satoshi Horikoshi[a], Kazuhiko Funabiki[b], Yasuhiko Tomino[a,*]

[a]*Division of Nephrology, Department of Internal Medicine, Juntendo University School of Medicine, Tokyo 113-8421, Japan*
[b]*Department of Nephrology and Hypertension, Juntendo Tokyo Koto Geriatric Medical Center, Tokyo 136-0075, Japan*
[c]*Sportology Center, Juntendo University Graduate School of Medicine, Tokyo 113-8421, Japan*

Received 27 August 2008; accepted 19 February 2009

Abstract

Advanced glycation end products (AGEs) contribute to the pathogenesis of diabetes-associated complications. Previously, we reported the possible effect of pyridoxamine (K-163), an AGE inhibitor, on improvement of glucose intolerance in type 2 diabetes mellitus KK-A^{y}/Ta mice. Recently, AGEs and oxidative stress have been shown to induce insulin resistance. The objective of the present study is to examine the effect of pyridoxamine on glucose intolerance and oxidative stress. C57BL/6J mice were divided into 3 groups as follows: low-fat diet, high-fat diet, and high-fat diet with pyridoxamine treatment. Body and adipose tissue weight, serum insulin, hydrogen peroxide, malondialdehyde and AGE, and urinary 8-hydroxy-2′-deoxyguanosine levels were measured. Nicotinamide adenine dinucleotide phosphate subunits, antioxidant enzymes, and adipocytokine messenger RNA expressions in the adipose tissues were evaluated. Akt/protein kinase B activity and glucose transporter 4 translocation in skeletal muscle were also evaluated. Body and adipose tissue weights of the pyridoxamine treatment group were significantly decreased compared with those of the high-fat diet group. Pyridoxamine attenuated serum hydrogen peroxide, malondialdehyde and AGE, and urinary 8-hydroxy-2′-deoxyguanosine and nicotinamide adenine dinucleotide phosphate oxidase expression; increased antioxidant enzyme expression; and improved dysregulation of adipocytokines in adipose tissues. Pyridoxamine improved blood glucose levels after glucose injection and fasting hyperinsulinemia. Suppressed Akt/protein kinase B activity and glucose transporter 4 translocation in skeletal muscle in high-fat diet mice were improved by pyridoxamine treatment. It appears that the antioxidative effect of pyridoxamine is associated with improvement of glucose intolerance and obesity in C57BL/6J mice fed a high-fat diet. We assume that pyridoxamine may be useful in the treatment of the obesity-associated metabolic syndrome.

1. Introduction

Advanced glycation/lipoxidation end products (AGEs/AGEs) are complex, heterogeneous, sugar/lipid-derived irreversible protein modifications that have been implicated in the pathogenesis of diabetic complications, atherosclerosis, and Alzheimer disease and in the process of normal aging [1,2].

Diabetes mellitus is closely associated with oxidative stress that could be a consequence of increased production of free radicals, reduced antioxidant defenses [3,4], or both. There is considerable evidence that hyperglycemia results in the generation of reactive oxygen species (ROS), ultimately leading to oxidative stress in various tissues. Another major source of reactive molecules, including superoxide and hydrogen peroxide (H_2O_2), is the enzyme nicotinamide adenine dinucleotide phosphate (NADPH) oxidase, which is activated by a variety of inflammatory cytokines [5,6]. Chronic activation of stress-sensitive signaling pathways by reactive molecules induces insulin resistance and impairs insulin secretion in vitro [7]. Oxidative stress has been linked to insulin resistance in vivo [8,9]. In a diabetic condition, oxidative stress impairs glucose uptake in muscles and fat [10,11]. More recent studies have found that this association is

* Corresponding author. Tel.: +81 3 5802 1064 or 1065; fax: +81 3 5802 1064 or 1065.
E-mail address: yasu@juntendo.ac.jp (Y. Tomino).

0026-0495/$ – see front matter © 2009 Elsevier Inc. All rights reserved.
doi:10.1016/j.metabol.2009.02.033

not restricted to insulin resistance in diabetes, but is also evident in obese, nondiabetic individuals [12,13] and in those with the metabolic syndrome [14,15]. If oxidative stress is causally linked to insulin resistance, it is reasonable to expect that treatment with antioxidants should have a beneficial impact on insulin sensitivity. There is evidence to support this idea in vitro, in animal models, and in clinical trials [16,17].

Adipocytes produce adipocytokines or adipokines, including plasminogen activator inhibitor–1 (PAI-1) [18], tumor necrosis factor–α (TNF-α) [19], leptin [20], and adiponectin [21]. Dysregulated production of these adipocytokines is involved in the pathogenesis of the obesity-associated metabolic syndrome. Increased production of PAI-1 and TNF-α from accumulated fat contributes to the development of insulin resistance [19] in obesity. In contrast, adiponectin exerts insulin-sensitizing [22,23] and antiatherogenic effects [24,25]; and hence, a decrease in plasma adiponectin is a causative factor in insulin resistance and atherosclerosis in obesity.

The effects of pyridoxamine include (*a*) inhibition of AGE formation by blocking oxidative degradation of the Amadori intermediate of the Millard reaction, (*b*) scavenging of toxic carbonyl products of glucose and lipid degradation, and (*c*) trapping of ROS [26]. Pyridoxamine inhibits AGE formation and retards the development of diabetic nephropathy in animal models for type 1 and type 2 diabetes mellitus [27,28]. Previously, we reported possible roles of pyridoxamine in improvement of impaired glucose tolerance and obesity in KK-A^y/Ta mice. However, the mechanisms of these effects are not clear [28].

In the present study, we aim to show that the antioxidative effect of pyridoxamine is associated with improvement of glucose intolerance and obesity in high-fat diet C57BL/6J mice.

2. Materials and methods

2.1. Animal studies

All animal care, procedures, and protocols were in accordance with the policies outlined in *The Guide for the Care and Handling of Laboratory Animals* (National Institutes of Health Publication No. 85-23), which was approved by the City of Hope National Medical Center Research Animal Care Committee. Male C57BL/6J mice (7 weeks of age) were purchased from CLEA Japan (Tokyo, Japan). Four mice were housed per plastic cage. All mice were maintained in the same room under conventional conditions with a regular 12-hour light/dark cycle and with temperature controlled at 24°C ± 1°C and given free access to water and food as described later.

2.2. Experimental design

The animals were randomly divided into the following 3 groups at 8 weeks of age: 8 mice were fed a low-fat diet for 12 weeks, 8 mice were fed a high-fat diet for 12 weeks, and 8 mice were fed a high-fat diet and given pyridoxamine 300 mg kg^{-1} d^{-1} in the drinking water for 12 weeks. The bioavailability of pyridoxamine is described in the "Discussion." The high-fat diet consisted of 58% lard (wt/wt), fish powder, 10% skim milk, and a 2% vitamin and mineral mixture (equivalent to 640 kcal/100 g; containing 7.5% carbohydrate, 24.5% protein, and 60% fat). The low-fat diet was equivalent to 348 kcal/100g, containing 48.4% carbohydrate, 27.8% protein, and 4.9% fat. Pyridoxamine dihydrochloride (K-163; 4-aminomethyl-3-hydroxyl-2-methyl-5-oxymethylpyridine dihydrochloride) was kindly provided by Kowa (Tokyo, Japan). C57BL/6J mice were killed after 10 minutes of glucose injection at 20 weeks of age. Adipose tissues from the inguinal, gonadal, mesenteric, and retroperitoneal regions; kidneys; and skeletal muscle were removed for RNA extraction, light microscopy, and immunoblot analysis. Lipid peroxidation was assessed by measuring malondialdehyde (MDA), an end product of fatty acid peroxidation.

2.3. Biochemical characterizations

Blood samples were obtained at each age by puncturing the ophthalmic venous plexus. Serum triglyceride and total cholesterol were also measured at 12, 16, and 20 weeks of age. Glucose tolerance was evaluated at 12 and 20 weeks of age. Serum fasting insulin levels, superoxide dismutase (SOD) activities, MDA concentration, H_2O_2 concentration, AGE concentration, urinary 8-hydroxy-2′-deoxyguanosine (8-OHdG), adipose tissue weight, and body height were measured at 20 weeks of age.

Serum total cholesterol and triglycerides were determined enzymatically by an autoanalyzer (Fuji Dry-Chem 5500; Fujifilm, Tokyo, Japan). Glucose tolerance was estimated by the intraperitoneal glucose tolerance test (IPGTT), which was performed by injection of glucose (2 g/kg in 20% solution) in overnight-fasted mice. Blood was obtained from the retroorbital sinus at 0 (fasting blood glucose level) and 120 minutes after intraperitoneal glucose injection for measurement of blood glucose and serum insulin levels. Glucose levels were measured using Glucocard (Kyoto Daiichi Kagaku, Kyoto, Japan). Serum insulin levels were measured by enzyme-linked immunosorbent assay (Insulin ELISA Kit; Morinaga, Tokyo, Japan). Serum MDA was determined colorimetrically using a commercial kit (Lipid Peroxidation Assay Kit; Calbiochem, San Diego, CA) according to the manufacturer's instructions. Serum H_2O_2 concentration was measured using an Amplex Red H_2O_2 assay kit (Invitrogen, Carlsbad, CA) according to the manufacturer's instructions. Serum SOD activity was also measured by enzyme immunoassay (SOD Assay Kit-WST; Dojindo Molecular Technologies, Tokyo, Japan). The SOD Assay Kit-WST assays SOD using WST-1 (2-[4-iodophenyl]-3-[4-nitrophenyl]-5-[2,4-disulfophenyl]-2H-tetrazolium, monosodium salt) that produces a water-soluble

formazan dye upon reduction with a superoxide anion. The rate of the reduction with $O2^-$ is linearly related to xanthine oxidase activity and is inhibited by SOD. The SOD activity was determined by inhibition of the rate of water-soluble formazan formation at 450 nm absorbance [29]. Serum AGE and urinary 8-OHdG levels were measured by enzyme-linked immunosorbent assay (SRL, Tokyo, Japan, and Fushimi Pharmaceutical, Kagawa, Japan).

2.4. Immunohistochemical staining

The kidneys were retrogradely perfused with saline via the abdominal aorta for 5 minutes at a pressure of about 150 mm Hg without prior flushing of the vasculature when the mice were killed at 20 weeks of age. Immunohistochemical analysis for carboxymethyl-lysine (CML) in renal tissue sections was performed using the ABC kit (Vector Laboratories, Burlingame, CA). Cryostat 3-μm kidney sections were air-dried for 10 minutes and then fixed in cold acetone for 10 minutes. To reduce the background, nonspecific binding was blocked by incubating with 10% normal goat serum in blocking solution (phosphate-buffered saline [pH 7.2] containing 2% bovine serum albumin, 2% fetal calf serum, and 0.2% fish gelatin) for 30 minutes. Nonspecific staining was blocked by incubation with avidin for 15 minutes and then biotin using the avidin-biotin blocking kit (Vector Laboratories). Endogenous peroxidase activity was inhibited by incubation with methanol containing 0.3% H_2O_2 for 10 minutes. The sections were then incubated with the primary antibody (Ab) diluted 1:100 in blocking solution at 4°C overnight. The primary Ab used in this study was anti-CML horseradish peroxidase conjugated (Trans Genic, Kumamoto, Japan). The sections were then incubated with a TSA Biotin System (PerkinElmer, Boston, MA) for 10 minutes. Biotinylated horseradish peroxidase was applied for 30 minutes. Peroxidase activity was developed in 3,3-diaminobenzidine. Finally, Mayer hematoxylin was added for counterstaining. Intensities of 3,3-diaminobenzidine in at least 20 glomeruli from each mouse were quantitated using the KS400 version 3.0 image analysis system (Carl Zeiss Vision, Munich, Germany). These examinations were performed by 2 investigators without knowledge of the origin of the slides, and the mean values were calculated [30,31].

2.5. Real-time reverse transcriptase polymerase chain reaction

NADPH oxidase complex consists of membrane-associated flavocytochrome b_{588} protein, which is composed of $gp91^{phox}$ and $p22^{phox}$, and cytosolic components $p47^{phox}$, $p67^{phox}$, and $p40^{phox}$. The messenger RNA (mRNA) expression of NADPH subunits, catalase, Cu-Zn-SOD, leptin, PAI-1, TNF-α, and adiponectin in white adipose tissue was estimated by quantitative real-time reverse transcriptase polymerase chain reaction (RT-PCR). Adipose tissues from the gonadal region were dissected out and then frozen in liquid nitrogen at 20 weeks of age. Samples were stored at −80°C before use. Total RNA from adipose tissues was extracted using Trizol (Life Technologies, Carlsbad, CA), and the purity was checked by spectrophotometry. To avoid contamination of genomic DNA, the samples were treated with DNase in all experiments. Isolated RNA (2 μg) was reverse-transcribed using random decamer primer (Ambion, Austin, TX) and M-MLV Reverse Transcriptase (Life Technologies). Quantitative PCR was performed using the SYBR Green PCR Master mix (PerkinElmer Applied Biosystems, Foster City, CA) and analyzed on an ABI PRISM 7500 Sequence Detector System (Perkin-Elmer Applied Biosystems). The forward and reverse primers used for each molecule were as follows: 5′-AACTT TGGCATTGTGGAAGG-3′ and 5′-GGATGCAGGGAT-GATGTTCT-3′ for mouse glyceraldehyde-3-phosphate dehydrogenase (GAPDH), 5′-GATGTTCCCCATT-GAGGCCG-3′ and 5′-GTTTCAGGTCATCAGGCCGC-3′ for mouse $p47^{phox}$, 5′-GCCGCTATCGCCAGTTCTAC-3′ and 5′-GCAGGCTCAGGAGGTTCTTC-3′ for mouse $p40^{phox}$, 5′-TTGGGTCAGCACTGGCTCTG-3′ and 5′-TGGCGGTGTGCAGTGCTATC-3′ for mouse $gp91^{phox}$, 5′-GTCCACCATGGAGCGATGTG-3′ and 5′-CAATGGC-CAAGCAGACGGTC-3′ for mouse $p22^{phox}$, 5′-CTGGCTGAGGCCATCAGACT-3′ and 5′-AGGCCACTG-CAGAGTGCTTG-3′ for mouse $p67^{phox}$, 5′-CAG-CATGGGTTCCACGTCCA-3′ and 5′-CACATT-GGCCACACCGTCCT-3′ for Cu-Zn-SOD, 5′-CCAGCGACCAGATGAAGCAG-3′ and 5′-CCACTCTCT-CAGGAATCCGC-3′ for catalase, 5′-AAGATCCCAGG-GAGGAAA-3′and 5′-CTGGTGGCCTTTGAAACT-3′ for leptin, 5′-TCAGCCCTTGCTTGCCTCAT-3′ and 5′-GCA-TAGCCAGCACCGAGGA-3′ for PAI-1, and 5′-GCCAC-CACGCTCTTCTG-3′ and 5′-GGTGTGGGTGAGGAGCA-3′ for TNF-α. Thermal cycling consisted of a denaturation step at 95°C for 10 minutes followed by 40 cycles at 95°C for 15 seconds and 40 cycles at 60°C for 1 minute. Amplification of specific transcripts was confirmed by melting curve profiles (cooling the sample to 60°C and heating slowly to 95°C with measurement of fluorescence) at the end of each PCR. Each data point measurement was repeated 4 times. The relative mRNA level in the sample was normalized to its GAPDH content. The data were expressed as the fold decrease in mRNA.

2.6. Immunoblot analysis

Isolation of membrane fractions and measurement of glucose transporter 4 (GLUT4) translocation in the isolated skeletal muscle were described previously [32]. Akt/protein kinase B (PKB) activity was also examined to assess insulin signaling of skeletal muscle. Sodium dodecyl sulfate polyacrylamide gel electrophoresis and immunoblot analyses were carried out according to standard protocols and visualized using enhanced chemiluminescence immunoblot

detection kits (Amersham Pharmacia Biotech, Little Chalfont, Buckinghamshire, United Kingdom). The primary Abs used in this study were as follows: rabbit anti-GLUT4 Ab (catalog no. AB1346; Chemicon International, Temecula, CA) and anti–phospho-Akt/PKB Ab (Cell Signaling Technology, Danvers, MA). Horseradish peroxidase–conjugated secondary Abs (Jackson Immunoresearch Laboratories, West Grove. PA) were used in this study. The optical density was measured by a Bio-Rad 5000 imaging system (Bio-Rad Laboratories, Hercules, CA).

2.7. Statistical analysis

All results are expressed as mean ± SEM. Comparisons among 3 or more parameters were analyzed by 1-way analysis of variance. P values less than .05 were considered as statistically significant.

3. Results

3.1. Characterization of mice

The phenotypic characterizations of high-fat diet C57BL/6J mice treated with or without pyridoxamine and low-fat diet C57BL/6J mice at different ages are shown in Table 1. Serum total cholesterol levels were significantly increased in high-fat diet mice at 12, 16, and 20 weeks of age ($P < .0001$). However, pyridoxamine significantly decreased serum total cholesterol levels of high-fat diet mice at 16 and 20 weeks of age ($P < .05$ and $P < .0001$, respectively). Serum triglyceride levels were significantly increased in high-fat diet mice at 12, 16, and 20 weeks of age ($P < .0001$), although pyridoxamine significantly decreased serum triglyceride levels of high-fat diet mice at 12, 16, and 20 weeks of age ($P < .05$). Individual food intakes (kilocalories per day) of mice fed a high-fat diet or a high-fat diet with pyridoxamine treatment were significantly higher than those of the low-fat diet mice. However, there were no significant differences between high-fat diet mice and pyridoxamine-treated mice. The mean levels of individual water intake (milliliters per day) were similar in the 3 groups.

Table 1
Characterization of high-fat diet mice with or without pyridoxamine

	Age (wk)	Low fat (n = 8)	High fat (n = 8)	Pyridoxamine (n = 8)
Serum total cholesterol (mmol/L)	12	2.9 ± 0.2	4.3 ± 0.2‡	4.4 ± 0.2‡
	16	2.5 ± 0.1	5.4 ± 0.2‡	4.4 ± 0.1†,‡
	20	2.6 ± 0.1	5.7 ± 0.2‡	4.7 ± 0.1‡,§
Serum triglyceride (mmol/L)	12	1.2 ± 0.1	1.7 ± 0.1‡	1.0 ± 0.1†
	16	1.4 ± 0.1	1.8 ± 0.1‡	1.4 ± 0.1†
	20	1.1 ± 0.0	1.7 ± 0.1‡	1.4 ± 0.0 *,†
Food intake (kcal/24 h)	20	10.79 ± 0.36	12.89 ± 0.42*	13.37 ± 0.81*
Water intake (mL/24 h)	20	2.61 ± 0.11	2.45 ± 0.13	2.58 ± 0.13

Data expressed as means ± SE.
* $P < .05$ vs low fat.
† $P < .05$ vs high fat.
‡ $P < .0001$ vs low fat.
§ $P < .0001$ vs high fat.

3.2. Effect of pyridoxamine on serum SOD activity, H_2O_2, MDA and AGE levels, and urinary 8-OHdG levels

Serum H_2O_2 was significantly increased in high-fat diet mice at 20 weeks of age ($P < .05$ vs low-fat diet mice). Pyridoxamine decreased the H_2O_2 levels ($P < .05$ vs high-fat diet mice) (Fig. 1A). Similarly, the mean level of serum MDA was higher in high-fat diet mice ($P < .05$ vs low-fat diet mice). The mean level of serum MDA in the pyridoxamine-treated group was significantly lower than that in the high-fat diet mice at 20 weeks of age ($P < .05$ vs high-fat diet mice). The SOD activities were significantly decreased in high-fat diet mice at 20 weeks of age ($P < .05$ vs low-fat diet mice). Pyridoxamine improved SOD activities of high-fat diet mice ($P < .05$ vs high-fat diet mice) (Fig. 1C). The mean level of serum AGE was higher in high-fat diet mice ($P < .05$ vs low-fat diet mice). However, the mean level of serum AGE in the pyridoxamine-treated group was significantly lower than that in the high-fat diet mice and low-fat diet mice ($P < .05$ vs high-fat diet and low-fat diet mice, respectively) (Fig. 1 D). Similarly, the mean level of urinary 8-OHdG was higher in high-fat diet mice ($P < .05$ vs low-fat diet mice). The mean level of urinary 8-OHdG in the pyridoxamine-treated group was significantly lower than that in the high-fat diet mice and low-fat diet mice ($P < .05$ vs high-fat diet and low-fat diet mice, respectively) (Fig. 1 E).

3.3. Effect of pyridoxamine on CML accumulation in glomeruli

The effect of pyridoxamine on CML accumulation in glomeruli was examined by immunostaining of CML. Carboxymethyl-lysine was hardly detected in glomeruli of low-fat diet mice (Fig. 2A). Accumulation of CML was found in glomeruli and expressed within mesangial areas of high-fat diet mice (Fig. 2B). Pyridoxamine treatment significantly decreased the accumulation of CML (Fig. 2C). No staining of CML was observed in the negative control without the primary Ab (Fig. 2D). The glomerular CML-stained area to whole glomerular area (WGA) ratio in the pyridoxamine-treated group was significantly lower than that in the high-fat diet group ($P < .0001$, Fig. 2E).

3.4. Effect of pyridoxamine on body weight and white adipose tissues

Body weights (BWs) of high-fat diet mice were significantly increased compared with those of control mice at 12, 16, and 20 weeks of age ($P = .033$, $P = .037$, and $P < .0001$). Although food intakes (kilocalories) did not differ between pyridoxamine-treated mice and high-fat diet mice, BWs of pyridoxamine-treated mice were significantly

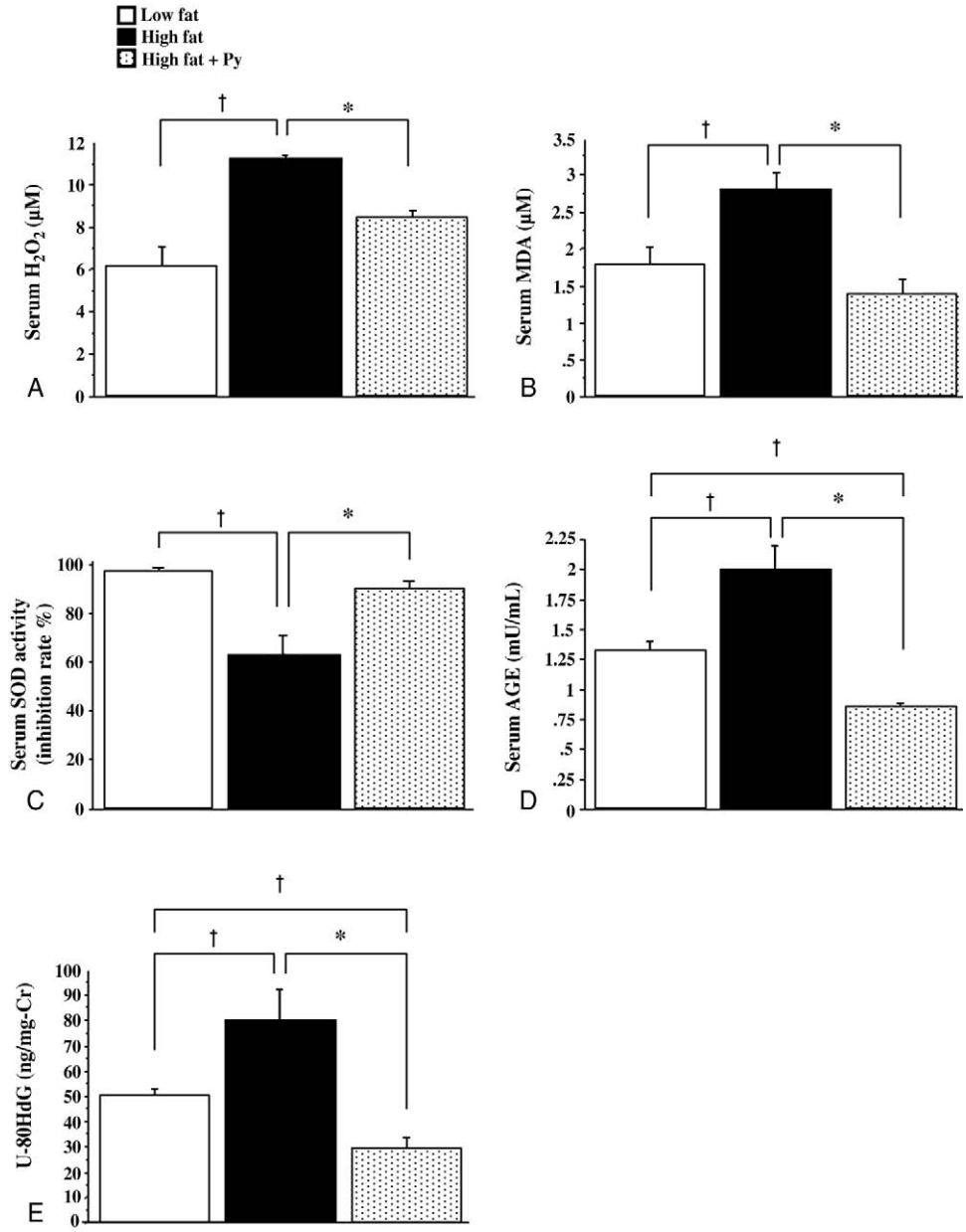

Fig. 1. Effect of pyridoxamine on serum oxidative stress and antioxidant enzyme. A, Serum H_2O_2 concentrations of low-fat diet, high-fat diet, and pyridoxamine-treated high-fat diet C57BL/6J mice at 20 weeks of age. B, Serum MDA concentrations of low-fat diet, high-fat diet, and pyridoxamine-treated high-fat diet C57BL/6J mice at 20 weeks of age. C, Serum SOD activity (inhibition rate, percentage) of low-fat diet, high-fat diet, and pyridoxamine-treated high-fat diet C57BL/6J mice at 20 weeks of age. D, Serum AGE concentrations of low-fat diet, high-fat diet, and pyridoxamine-treated high-fat diet C57BL/6J mice at 20 weeks of age. E, Urinary 8-OHdG levels of low-fat diet, high-fat diet, and pyridoxamine-treated high-fat diet C57BL/6J mice at 20 weeks of age. Data expressed as mean ± SE (n =8). $^{\dagger}P < .05$ vs low fat, $^{*}P < .05$ vs high fat. Py indicates pyridoxamine.

decreased compared with those of high-fat diet mice at 16 and 20 weeks of age ($P = .044$ and $P = .0012$) (Fig. 3A). Adipose tissues of the inguinal, gonadal, mesenteric, and retroperitoneal regions in high-fat diet mice were significantly increased compared with those of control mice at 20 weeks of age ($P < .0001$, $P < .0001$, $P = .0003$, and $P < .0001$). However, adipose tissues of the inguinal, gonadal, mesenteric, and retroperitoneal regions in pyridoxamine-treated mice were significantly decreased compared with those of high-fat mice ($P = .0014$, $P < .0001$, $P = .0061$, and $P < .0001$) (Fig. 3B).

3.5. Effect of pyridoxamine on mRNA expression of NADPH oxidase and adipocytokines in white adipose tissues

The results showed that mRNA expressions of $P47^{phox}$, $gp91^{phox}$, $p40^{phox}$, $p22^{phox}$, and $p67^{phox}$ in adipose tissues were significantly elevated in the high-fat diet group ($P =$

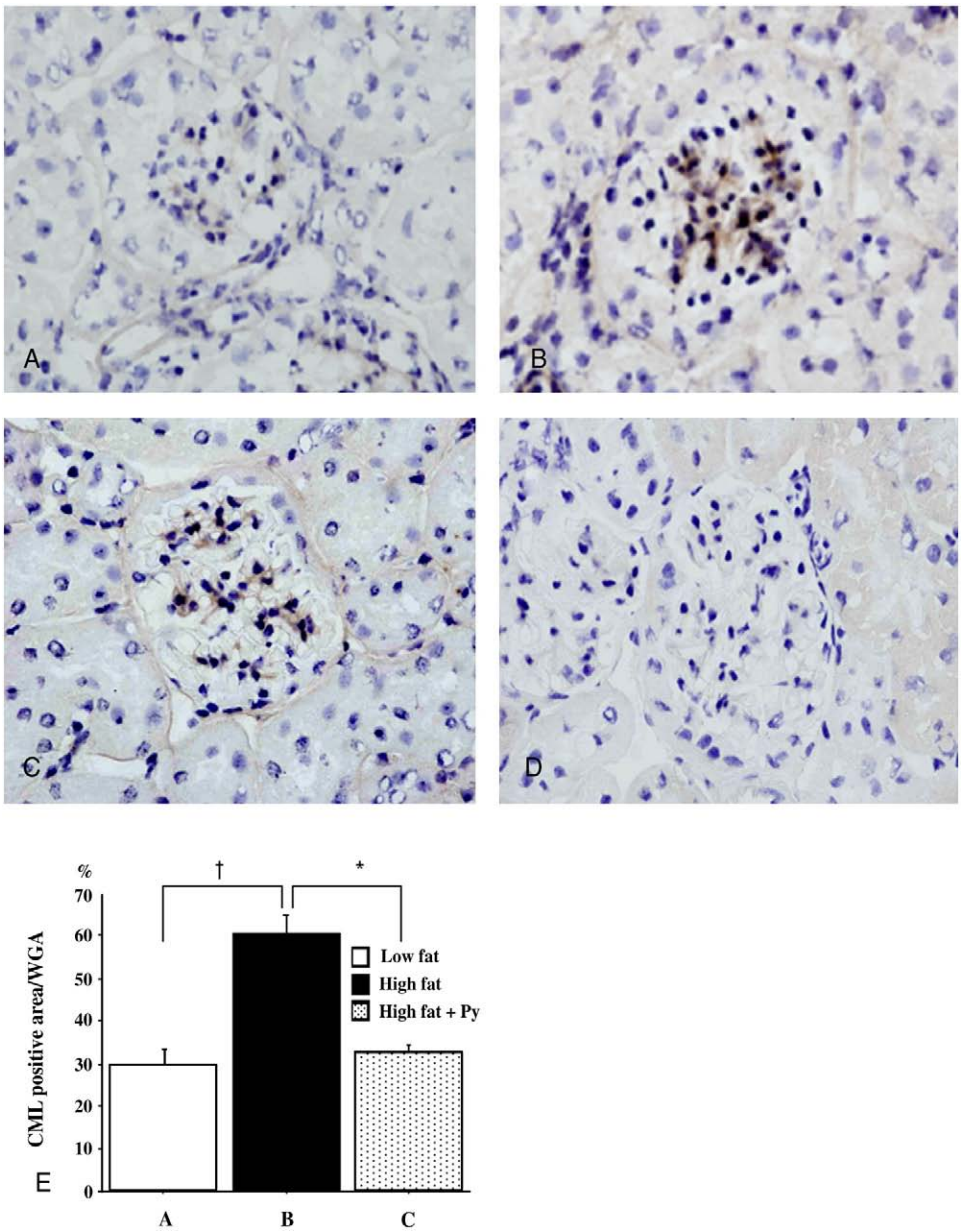

Fig. 2. Representative immunohistochemical staining for CML at 20 weeks of age in renal tissue sections treated with pyridoxamine. A, Carboxymethyl-lysine was hardly observed in the glomeruli and extraglomerular arterial walls of low-fat diet group. B, Accumulation of CML was observed in the glomeruli of high-fat diet group. C, Accumulation of CML was decreased in the glomeruli of high-fat diet with pyridoxamine treatment group. D, No staining of CML was observed in the negative control without the primary Ab. E, Quantification of CML accumulation in the glomeruli of the 3 groups. Original magnification: ×400. Data expressed as mean ± SE. $^{\dagger}P < .0001$ vs low fat, $^{*}P < .0001$ vs high fat. WGA indicates whole glomerular area.

.001, $P < .0001$, $P = .0025$, $P = .0045$, and $P = .0002$, respectively). However, pyridoxamine decreased these mRNA expressions ($P = .002$, $P < .0001$, $P = .0048$, and $P = .0027$) (Fig. 4A-E). Catalase and Cu-Zn-SOD mRNA expressions were significantly decreased in the high-fat diet group ($P = .0111$ and $P = .0034$), and pyridoxamine increased these mRNA expressions ($P = .0423$ and $P = .0304$) (Fig. 4F-G). Furthermore, mRNA expressions of leptin, TNF-α, and PAI-1 in adipose tissues were significantly elevated in the high-fat diet group ($P < .0001$, $P = .0014$, and $P = .0062$); and pyridoxamine decreased these mRNA expressions ($P < .0001$, $P = .0029$, and $P = .0044$) (Fig. 5A-C). On the other hand, adiponectin mRNA expression was significantly decreased in the high-fat diet group ($P = .0063$); and pyridoxamine increased such mRNA expression ($P = .0234$) (Fig. 5D).

3.6. Effect of pyridoxamine on impaired glucose tolerance and hyperinsulinemia

To examine changes in impaired glucose tolerance, IPGTT was performed at 12 and 20 weeks of age. As

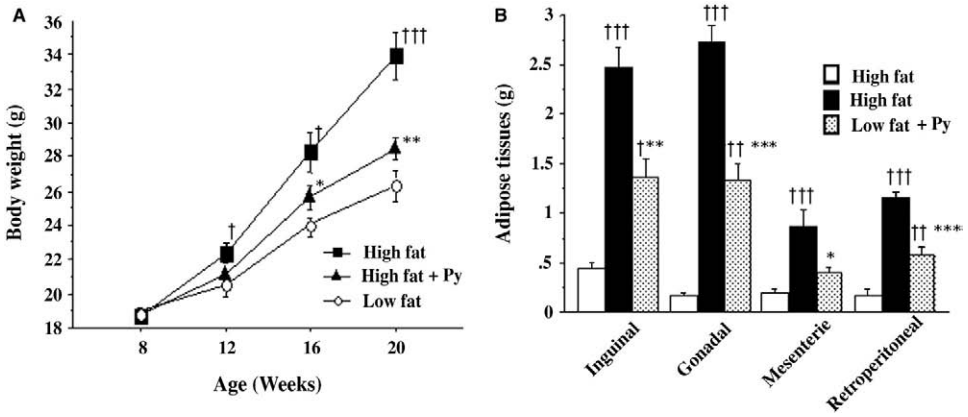

Fig. 3. Mean BWs and adipose tissue weights of C57BL/6J mice. A, Body weights of high-fat diet mice were significantly increased compared with those of low-fat diet mice; but BWs of pyridoxamine-treated mice were significantly decreased compared with those of high-fat diet mice at 12, 16, and 20 weeks of age. B, Adipose tissues of inguinal, gonadal, mesenteric, and retroperitoneal regions of high-fat diet mice were significantly increased compared with those of low-fat diet mice. However, those of pyridoxamine-treated mice were significantly decreased compared with those of high-fat diet mice at 20 weeks of age. Data expressed as mean ± SE. $^{\dagger}P$ less than .05 vs low fat, $^{\dagger\dagger}P < .005$ vs low fat, $^{\dagger\dagger\dagger}P < .0005$ vs low fat, $*P < .05$ vs high fat, $**P < .005$ vs high fat, and $***P < .0005$ vs high fat.

shown in Fig. 6A, blood glucose was significantly increased in 12-week–old high-fat diet mice at 30 and 60 minutes compared with control mice ($P < .0005$). However, glucose tolerance was significantly improved in pyridoxamine-treated mice ($P < .005$). Glucose intolerance was more severe in 20-week–old high-fat diet mice; and pyridoxamine significantly improved blood glucose levels at 30, 60, and 120 minutes ($P < .005$, $P < .05$, and $P < .005$) (Fig. 6B). As shown in Fig. 6C, fasting serum insulin levels were significantly increased in 20-week–old high-fat diet mice compared with control mice ($P < .05$); and pyridoxamine significantly improved hyperinsulinemia ($P < .05$).

3.7. Effect of pyridoxamine on Akt/PKB activity and GLUT4 translocation in skeletal muscle

Akt/PKB activity and GLUT4 translocation in skeletal muscle were estimated by Western blot analysis. Phosphorylated Akt/PKB of cytoplasm and GLUT4 in plasma membrane of skeletal muscle were significantly suppressed in the high-fat diet group at 10 minutes after injection of glucose ($P = .0002$ and $P = .0002$). However, pyridoxamine significantly improved these activities ($P = .002$ and $P = .002$) (Fig. 7A, B).

4. Discussion

In the present study, we demonstrated that pyridoxamine, an AGE inhibitor, improved glucose intolerance; suppressed serum H_2O_2, MDA, AGE, and urinary 8-OHdG levels; reduced mRNA expression of NADPH subunits; increased antioxidative enzymes in white adipose tissues; and improved insulin signaling of skeletal muscle in high-fat diet C57BL/6J mice. Furthermore, pyridoxamine decreased the BW and adipose tissues. There were no significant differences in the levels of mean blood pressure, fasting blood glucose hemoglobin A_{1c} (HbA_{1c}) and urinary albumin-creatinine ratio (ACR), urinary volume, and stool weight among the 3 groups at all ages. Urinary glucose was negative in all mice of the 3 groups at all ages (data not shown).

Previously, we reported the effect of pyridoxamine (K-163) on type 2 diabetes mellitus nephropathy in KK-A^y/Ta mice given pyridoxamine at 200 or 400 mg. In the 200–mg kg^{-1} d^{-1} treatment group, pyridoxamine improved the levels of urinary ACR and accumulation of CML in renal section without changing BW, casual blood glucose, and HbA_{1c}. In the 400–mg kg^{-1} d^{-1} treatment group, pyridoxamine prevented not only urinary ACR and CML accumulation but also increase of BW, casual blood glucose, and HbA_{1c} [28]. It is postulated that the effect of treatment at 200 vs 400 mg kg^{-1} d^{-1} on these parameters might be related to antioxidant effects by pyridoxamine; and large doses of pyridoxamine have effects such as improvement of BW gain and glucose intolerance. Although the water-soluble B vitamins are often considered to be nontoxic, pyridoxine is especially toxic to the peripheral nervous system [33]. Pyridoxine is interconvertible in vivo with the vitamers pyridoxal and pyridoxamine [34]. Pyridoxamine was significantly less toxic, which made it possible to study effects after doses that matched or exceeded the doses of pyridoxine [35]. The better bioavailability of pyridoxamine and its low toxicity (5000-7500 mg/kg oral LD_{50} in rodents) [36], combined with its more pronounced effects on renal disease, hyperlipidemia, and metabolic changes, suggest that pyridoxamine may be useful for clinical treatment of a wide range of diabetic complications including vascular disease and nephropathy [27]. It was suggested that the doses of pyridoxamine used in this study were not toxic.

We have shown that pyridoxamine decreased systemic oxidative stress estimated by serum H_2O_2, MDA, AGE, and urinary 8-OHdG, a marker of oxidative DNA damage, in high-fat diet C57BL/6J mice. The carboxyl group of

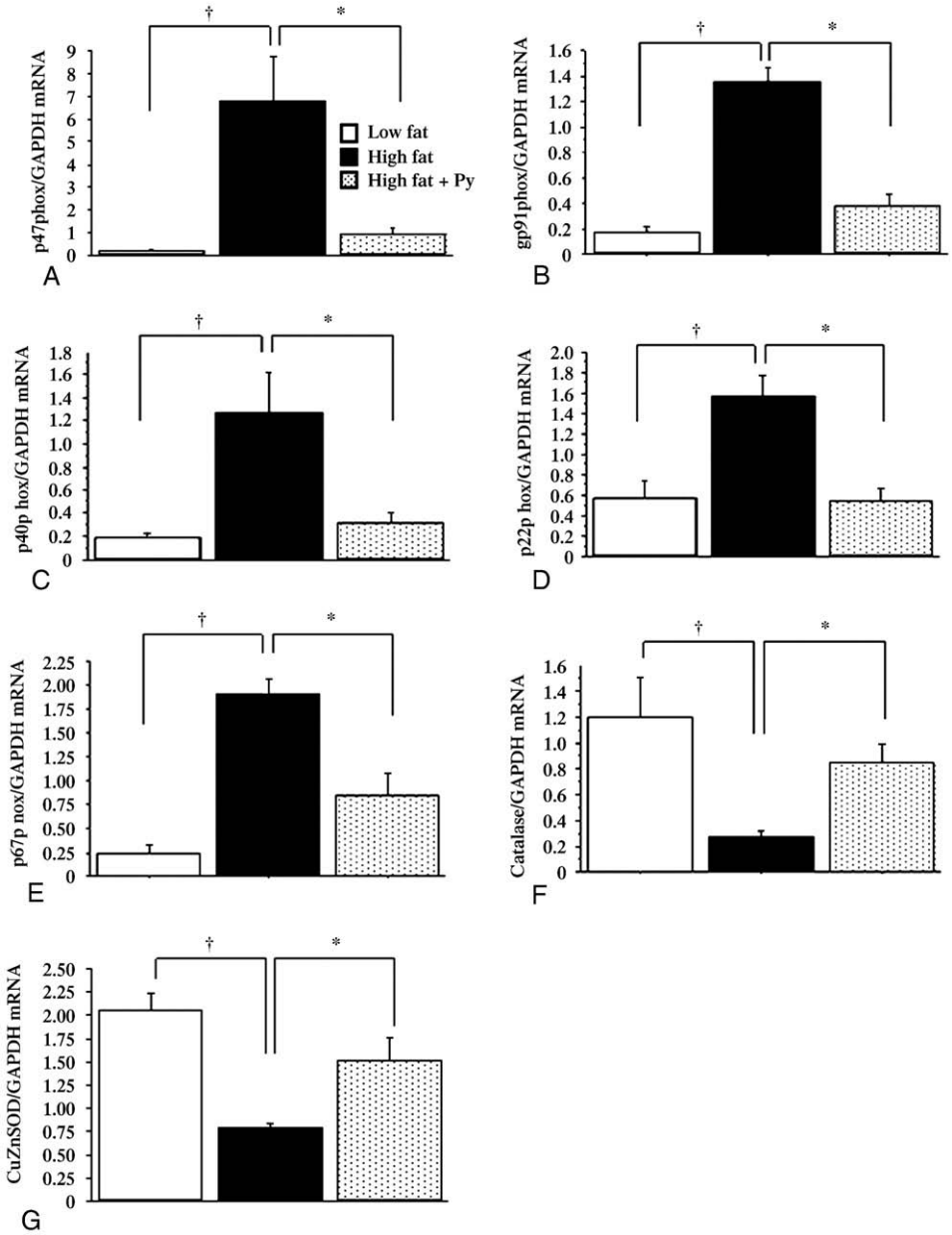

Fig. 4. Messenger RNA expression of NADPH subunits and antioxidant estimated by real-time RT-PCR in adipose tissues of C57BL/6J mice at 20 weeks of age. $P47^{phox}$ (A), $gp91^{phox}$ (B), $p40^{phox}$ (C), $p22^{phox}$ (D), $p67^{phox}$ (E), catalase (F), and Cu-Zn-SOD (G) mRNA expressions were normalized to GAPDH mRNA content. Bar graph shows mean ± SE from 8 mice in each group, expressed as fold over control. $^{\dagger}P < .05$ vs low fat, $^{*}P < .05$ vs high fat. Py indicates pyridoxamine.

pyridoxamine can bind to the ε-amino group of a lysine residue, forming a Schiff base or aldimine. Previous observations clearly showed that pyridoxamine acts as a sacrificial nucleophile, trapping reactive intermediates in lipoxidation and glycoxidation reactions [37]. Oxidative stress is linked to the pathogenesis and pathobiochemistry of various diseases, including cancer, diabetes, and cardiovascular diseases. The nonspecific harmful effect of ROS generated during oxidative stress is involved in the development of disease, as well as the activation of a specific signaling cascade of the cell exposed to higher oxidative load. The interaction of ROS with the insulin signaling pathway may occur at several levels [38].

We speculate that pyridoxamine ameliorates insulin sensitivity via suppression of oxidative stress and AGE formation. It has been reported that prolonged exposure of 3T3-L1 adipocytes to ROS results in impairment of insulin-induced activation of phosphoinositide 3-kinase and Akt/PKB, insulin-stimulated lipogenesis, glucose uptake, and GLUT 4 translocation to the plasma membrane [11,39]. *S*-nitrosylation of Akt/PKB-mediated inactivation is considered to contribute to the pathogenesis of inducible nitric

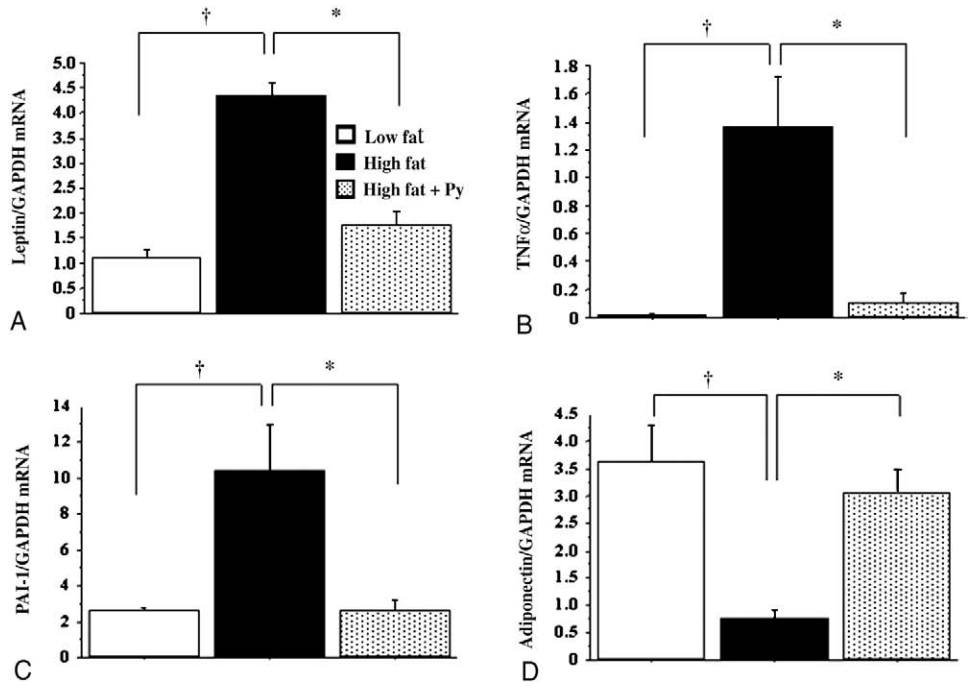

Fig. 5. Messenger RNA expression of adipocytokines estimated by real-time RT-PCR in adipose tissues of C57BL/6J mice at 20 weeks of age. Leptin (A), TNF-*a* (B), PAI-1 (C), and adiponectin (D) mRNA expressions were normalized to GAPDH mRNA content. Bar graph shows mean ± SE from 8 mice in each group, expressed as fold over control. $^{\dagger}P < .05$ vs low fat, $*P < .05$ vs high fat. Py indicates pyridoxamine.

oxide synthase– and/or oxidative stress–involved insulin resistance [40]. Several previous studies demonstrated that antioxidant treatment improves insulin function in diabetic subjects [16,41]. In streptozotocin-diabetic hamsters, pyridoxamine reduced oxidative stress as measured by plasma 8-OHdG and MDA plus 4-hydroxy-2-noneal levels and

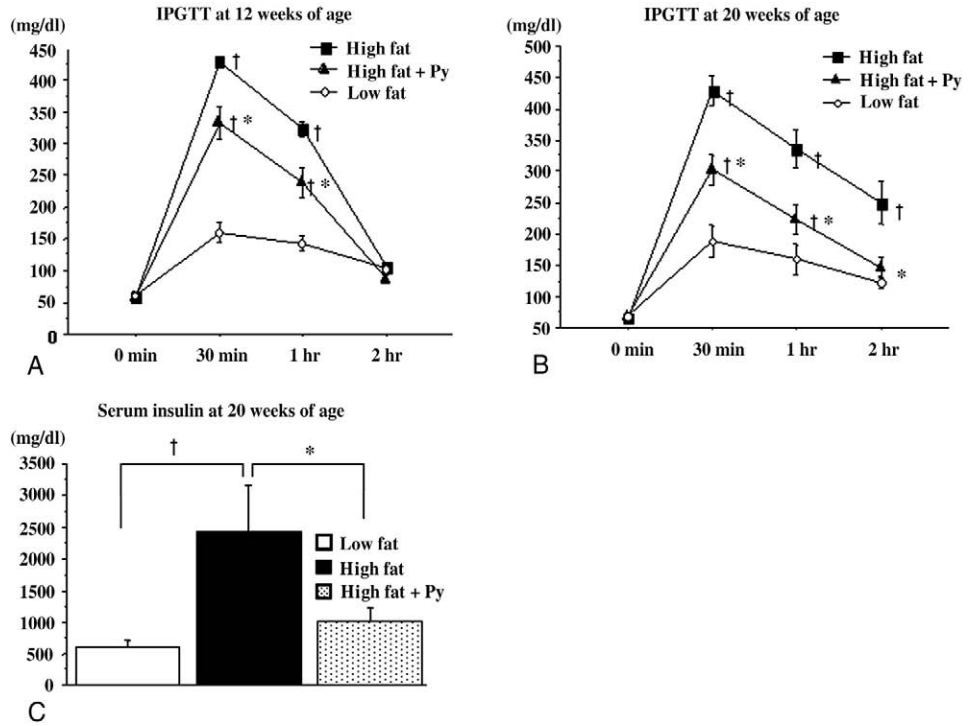

Fig. 6. Effect of pyridoxamine on impaired glucose tolerance and hyperinsulinemia. Blood glucose levels in the IPGTT at 12 weeks (A) and 20 weeks (B) of age. C, Serum insulin levels at 20 weeks of age. Data expressed as mean ± SE. $^{\dagger}P < .05$ vs low fat, $*P < .05$ vs high fat. Py indicates pyridoxamine.

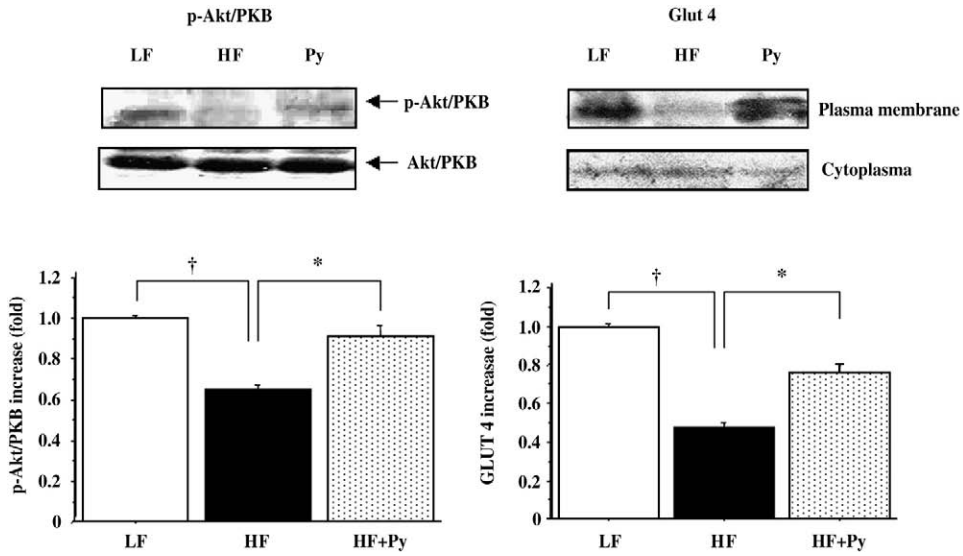

Fig. 7. Effect of pyridoxamine on Akt/PKB activity and GLUT4 translocation in skeletal muscle. Whole cell lysate was prepared and normalized to equal protein concentration and analyzed by Western blotting using Abs to p-Akt/PKB and Akt/PKB (A). Whole cell lysate and plasma membrane fractions were prepared, normalized to equal protein concentration, and analyzed by Western blotting using Abs to GLUT 4 (B). The values were quantified using a densitometer. Data expressed as mean ± SE. $^{\dagger}P < .05$ vs low fat, $^{*}P < .05$ vs high fat. LF indicates low fat; HF, high fat; Py, pyridoxamine.

restored β-cell function [42]. Miele et al [43] reported that human glycated albumin induces resistance to insulin at the insulin receptor substrate level by activating the protein kinase C-α isoform. They noted that AGE may participate in the development of insulin resistance. Kuniyasu et al [44] reported that AGE-modified bovine serum albumin was endocytosed by adipocytes via CD36. Their results suggested that CD36-mediated interaction of AGE-modified proteins with adipocytes might play a pathologic role in obesity or insulin resistance. We showed that the mean levels of serum AGE and urinary 8-OHdG were significantly lower in the pyridoxamine treatment group than in the low-fat diet group, although BW gain showed no difference between the 2 groups. These results indicate that changes observed in the pyridoxamine-treated mice were related to the antioxidant effect of pyridoxamine rather than to functional caloric restriction.

We demonstrated that mRNA expression of NADPH oxidase was decreased and antioxidative enzymes were increased by pyridoxamine treatment. Furthermore, mRNA expression of adipocytokines was improved by pyridoxamine treatment. Furukawa et al [45] reported that increased oxidative stress in accumulated fat via increased NADPH oxidase and decreased antioxidant enzymes causes local dysregulated production of adipocytokines. Increased ROS production from accumulated fat also leads to an increase in oxidative stress in blood, affecting other organs including the liver, skeletal muscle, and aorta. They demonstrated that ROS production of 3T3-L1 adipocytes was increased, in parallel with fat accumulation, by incubation with linolenic acid in an NADPH oxidase-dependent manner [45]. It seems that down-regulation of NADPH oxidase and up-regulation of antioxidant enzyme are not direct effects of pyridoxamine but the results of decreased fat accumulation and ROS production by pyridoxamine treatment.

It is difficult to clarify the mechanism of decrease in BW and adipose tissue weight in the pyridoxamine-treated group in this study, but improvement of insulin sensitivity by pyridoxamine may be related to the mechanism. The possibility of the loss of calories by gastrointestinal malabsorption, pyridoxamine toxicity, and glycosuria in the pyridoxamine group is unlikely because we confirmed no difference in weight of stool and urinary volume among the 3 groups, negative glycosuria, and bioavailability of pyridoxamine. Gronning et al [46] reported that insulin and TNF-α regulate the expression of Foxc2, which is the winged helix/forkhead gene that regulates adipocyte metabolism counteracting obesity and diet-induced insulin resistance. Foxc2 mRNA is up-regulated in wild-type mice fed a high-fat diet when compared with standard diet, indicating that Foxc2 is regulated in response to diet energy content. After Foxc2 levels were elevated, the metabolic rate increased in the sense that excess calories showed an increased tendency to dissipate heat rather than being stored as triglyceride droplets. By long-term stimulation with TNF-α or insulin, which mimics the conditions in obesity and/or insulin resistance, the regulation of Foxc2 is terminated; and Foxc2 mRNA is at basal levels. Thus, improvement of insulin resistance and decreased TNF-α production by antioxidative effects of pyridoxamine could improve dysregulation of the expression of Foxc2 and increase adipocyte metabolic rate. Another possible mechanism of decreased fat accumulation by pyridoxamine may be due to improved dysregulation of lipolysis by the cyclic adenosine monophosphate (cAMP) pathway in adipocytes. Cyclic adenosine monophosphate production is modulated by hormone receptors coupled to

the Gs/Gi family of guanosine triphosphate binding proteins, such as β-adrenergic receptors, whereas cAMP degradation is controlled by modulation of phosphodiesterase activity, increased by insulin receptor signaling. Cyclic adenosine monophosphate activates protein kinase A, which activates hormone-sensitive lipase by promoting its phosphorylation. Hormone-sensitive lipase is the enzyme that hydrolyzes intracellular triacylglycerol and diacylglycerol, and is one of the key molecules controlling lipolysis [47]. Thus, it is postulated that improved insulin sensitivity via suppression of oxidative stress by pyridoxamine could improve dysregulated lipolysis by the cAMP–hormone-sensitive lipase pathway. Further studies of the effects of pyridoxamine on fat accumulation are warranted.

In conclusion, it appears that the antioxidative effect of pyridoxamine is associated with improvement of glucose intolerance and fat accumulation in high-fat diet C57BL/6J mice. We propose that pyridoxamine may be useful against the obesity-associated metabolic syndrome.

Acknowledgment

We thank Kowa (Tokyo, Japan) for providing K-163. We also thank Ms Terumi Shibata, Dr Mariko Tamano, Mr Yoshihiro Kubota, and Ms Mayumi Ishiwata for their skillful technical support and advice. This study was partly supported by High Technology Research Center Grant from the Ministry of Education, Culture, Sports, Science, and Technology of Japan.

References

[1] Brownlee M. Advanced protein glycosylation in diabetes and aging. Annu Rev Med 1995;46:223-34.
[2] Vlassara H, Palace MR. Diabetes and advanced glycation endproducts. J Intern Med 2002;251:87-101.
[3] Rösen P, Nawroth PP, King G, Möller W, Tritschler HJ, Packer L. The role of oxidative stress in the onset and progression of diabetes and its complications: a summary of a Congress Series sponsored by UNESCO-MCBN, the American Diabetes Association and the German Diabetes Society. Diabetes Metab Res Rev 2001;17:189-212.
[4] West IC. Radicals and oxidative stress in diabetes. Diabet Med 2000; 17:171-80.
[5] Dröge W. Free radicals in the physiological control of cell function. Physiol Rev 2002;82:47-95.
[6] Zalba G, San José G, Moreno MU, et al. Oxidative stress in arterial hypertension: role of NAD(P)H oxidase. Hypertension 2001;38: 1395-9.
[7] Evans JL, Goldfine ID, Maddux BA, Grodsky GM. Are oxidative stress–activated signaling pathways mediators of insulin resistance and beta-cell dysfunction? Diabetes 2003;52:1-8.
[8] Bruce CR, Carey AL, Hawley JA, Febbraio MA. Intramuscular heat shock protein 72 and heme oxygenase-1 mRNA are reduced in patients with type 2 diabetes: evidence that insulin resistance is associated with a disturbed antioxidant defense mechanism. Diabetes 2003;52: 2338-45.
[9] Ceriello A. Oxidative stress and glycemic regulation. Metabolism 2000;49:27-9.
[10] Maddux BA, See W, Lawrence Jr JC, Goldfine AL, Goldfine ID, Evans JL. Protection against oxidative stress-induced insulin resistance in rat L6 muscle cells by micromolar concentrations of alpha-lipoic acid. Diabetes 2001;50:404-10.
[11] Rudich A, Tirosh A, Potashnik R, Hemi R, Kanety H, Bashan N. Prolonged oxidative stress impairs insulin-induced GLUT4 translocation in 3T3-L1 adipocytes. Diabetes 1998;47:1562-9.
[12] Smith SR, Bai F, Charbonneau C, Janderova L, Argyropoulos G. A promoter genotype and oxidative stress potentially link resistin to human insulin resistance. Diabetes 2003;52:1611-8.
[13] Urakawa H, Katsuki A, Sumida Y, et al. Oxidative stress is associated with adiposity and insulin resistance in men. J Clin Endocrinol Metab 2003;88:4673-6.
[14] Ford ES, Mokdad AH, Giles WH, Brown DW. The metabolic syndrome and antioxidant concentrations: findings from the Third National Health and Nutrition Examination Survey. Diabetes 2003;52: 2346-52.
[15] Hitsumoto T, Iizuka T, Takahashi M, et al. Relationship between insulin resistance and oxidative stress in vivo. J Cardiol 2003;42: 119-27.
[16] Evans JL, Goldfine ID, Maddux BA, Grodsky GM. Oxidative stress and stress-activated signaling pathways: a unifying hypothesis of type 2 diabetes. Endocr Rev 2002;23:599-622.
[17] Evanz JL, Maddux BA, Goldfine ID. Antioxidants in diabetic complications and insulin resistance. In: Pickup Raz I, Skyler JS, Shafrir E, editors. Diabetes: from research to diagnosis and treatment. London: Martin Dunitz; 2003. p. 479-96.
[18] Shimomura I, Funahashi T, Takahashi M, et al. Enhanced expression of PAI-1 in visceral fat: possible contributor to vascular disease in obesity. Nat Med 1996:800-3.
[19] Uysal KT, Wiesbrock SM, Marino MW, Hotamisligil GS. Protection from obesity-induced insulin resistance in mice lacking TNF-alpha function. Nature 1997;389:610-4.
[20] Unger RH. The physiology of cellular liporegulation. Annu Rev Physiol 2003;65:333-47.
[21] Matsuzawa Y, Funahashi T, Kihara S, Shimomura I. Adiponectin and metabolic syndrome. Arterioscler Thromb Vasc Biol 2004;24: 29-33.
[22] Fruebis J, Tsao TS, Javorschi S, et al. Proteolytic cleavage product of 30-kDa adipocyte complement-related protein increases fatty acid oxidation in muscle and causes weight loss in mice. Proc Natl Acad Sci U S A 2001;98:2005-10.
[23] Yamauchi T, Kamon J, Waki H, et al. The fat-derived hormone adiponectin reverses insulin resistance associated with both lipoatrophy and obesity. Nat Med 2001;7:941-6.
[24] Okamoto Y, Kihara S, Ouchi N, et al. Adiponectin reduces atherosclerosis in apolipoprotein E–deficient mice. Circulation 2002; 106:2767-70.
[25] Yamauchi T, Kamon J, Waki H. Globular adiponectin protected *ob*/*ob* mice from diabetes and ApoE-deficient mice from atherosclerosis. J Biol Chem 2003;278:2461-8.
[26] Voziyan PA, Hudson BG. Pyridoxamine as a multifunctional pharmaceutical: targeting pathogenic glycation and oxidative damage. Cell Mol Life Sci 2005;62:1671-81.
[27] Degenhardt TP, Alderson NL, Arrington DD, Beattie RJ, Basgen JM, Steffes MW. Pyridoxamine inhibits early renal disease and dyslipidemia in the streptozotocin-diabetic rat. Kidney Int 2002;61: 939-50.
[28] Tanimoto M, Gohda T, Kaneko S, Hagiwara S, Murakoshi M, Aoki T, et al. Effect of pyridoxamine (K-163), an inhibitor of advanced glycation end products, on type 2 diabetic nephropathy in KK-A(y)/Ta mice. Metabolism 2007;56:160-7.
[29] Ukeda H, Kawana D, Maeda S, Sawamura M. Spectrophotometric assay for superoxide dismutase based on the reduction of highly water-soluble tetrazolium salts by xanthine-xanthine oxidase. Biosci Biotechnol Biochem 1999;63:485-8.
[30] Ito T, Tanimoto M, Yamada K, et al. Glomerular changes in the KK-Ay/Ta mouse: a possible model for human type 2 diabetic nephropathy. Nephrology (Carlton) 2006;11:29-35.

[31] Zhang M, Hagiwara S, Matsumoto M, et al. Effects of eicosapentaenoic acid on the early stage of type 2 diabetic nephropathy in KKA(y)/Ta mice: involvement of anti-inflammation and antioxidative stress. Metabolism 2006;55:1590-8.
[32] Ogihara T, Asano T, Ando K, et al. Angiotensin II-induced insulin resistance is associated with enhanced insulin signaling. Hypertension 2002;40:872-9.
[33] Jortner BS. Mechanisms of toxic injury in the peripheral nervous system: neuropathologic considerations. Toxicol Pathol 2000;28:54-69 [Review].
[34] McCormick DB, Chen H. Update on interconversions of vitamin B-6 with its coenzyme. J Nutr 1999;129:325-7 [Review].
[35] Levine S, Saltzman A. Pyridoxine (vitamin B6) neurotoxicity: enhancement by protein-deficient diet. J Appl Toxicol 2004;24:497-500.
[36] Materials safety data sheet, product #P9380 (pyridoxamine dihydrochloride). St. Louis, Sigma-Aldrich Chemical Co.
[37] Onorato JM, Jenkins AJ, Thorpe SR, Baynes JW. Pyridoxamine, an inhibitor of advanced glycation reactions, also inhibits advanced lipoxidation reactions. Mechanism of action of pyridoxamine. J Biol Chem 2000;275:21177-84.
[38] Erol A. Insulin resistance is an evolutionarily conserved physiological mechanism at the cellular level for protection against increased oxidative stress. Bioessays 2007;29:811-8.
[39] Tirosh A, Potashnik R, Bashan N, Rudich A. Oxidative stress disrupts insulin-induced cellular redistribution of insulin receptor substrate–1 and phosphatidylinositol 3-kinase in 3T3-L1 adipocytes. A putative cellular mechanism for impaired protein kinase B activation and GLUT4 translocation. J Biol Chem 1999;274:10595-602.
[40] Yasukawa T, Tokunaga E, Ota H, Sugita H, Martyn JA, Kaneki M. *S*-nitrosylation–dependent inactivation of Akt/protein kinase B in insulin resistance. J Biol Chem 2005;280:7511-8.
[41] Jacob S, Ruus P, Hermann R, et al. Oral administration of RAC-alpha-lipoic acid modulates insulin sensitivity in patients with type-2 diabetes mellitus: a placebo-controlled pilot trial. Free Radic Biol Med 1999;27:309-14.
[42] Takatori A, Ishii Y, Itagaki S, Kyuwa S, Yoshikawa Y. Amelioration of the beta-cell dysfunction in diabetic APA hamsters by antioxidants and AGE inhibitor treatments. Diabetes Metab Res Rev 2004;20:211-8.
[43] Miele C, Riboulet A, Maitan MA, Oriente F, Romano C, Formisano P, et al. Human glycated albumin affects glucose metabolism in L6 skeletal muscle cells by impairing insulin-induced insulin receptor substrate (IRS) signaling through a protein kinase C alpha–mediated mechanism. J Biol Chem 2003;278:47376-87.
[44] Kuniyasu A, Ohgami N, Hayashi S, Miyazaki A, Horiuchi S, Nakayama H. CD36-mediated endocytic uptake of advanced glycation end products (AGE) in mouse 3T3-L1 and human subcutaneous adipocytes. FEBS Lett 2003;537:85-90.
[45] Furukawa S, Fujita T, Shimabukuro M, et al. Increased oxidative stress in obesity and its impact on metabolic syndrome. J Clin Invest 2004;114:1752-61.
[46] Grønning LM, Cederberg A, Miura N, Enerbäck S, Taskén K. Insulin and TNF alpha induce expression of the forkhead transcription factor gene Foxc2 in 3T3-L1 adipocytes via PI3K and ERK 1/2-dependent pathways. Mol Endocrinol 2002;16:873-83.
[47] Carmen GY, Víctor SM. Signalling mechanisms regulating lipolysis. Cell Signal 2006;18:401-8.